Generalized Drude–Lorentz Model Complying with the Singularity Expansion Method

Isam Ben Soltane, Félice Dierick, Brian Stout, Nicolas Bonod

ADVANCED OPTICAL MATERIALS
www.advopticalmat.de

Generalized Drude–Lorentz Model Complying with the Singularity Expansion Method

Isam Ben Soltane, Félice Dierick, Brian Stout, and Nicolas Bonod**

Deriving analytical expressions of dielectric permittivities is required for numerical and physical modeling of optical systems and the soar of non-Hermitian photonics motivates their prolongation in the complex plane. Analytical models are based on the association of microscopic models to describe macroscopic effects. However, the question is to know whether the resulting Debye–Drude–Lorentz models are not too restrictive. Here, it is shown that the permittivity must be treated as a meromorphic transfer function that complies with the requirements of complex analysis. This function can be naturally expanded on a set of complex singularities. This singularity expansion of the dielectric permittivity allows to derive a generalized expression of the Debye–Drude–Lorentz model that complies with the requirements of complex analysis and the constraints of physical systems. It is shown that the complex singularities and other parameters of this generalized expression can be retrieved from experimental data acquired along the real frequency axis. The accuracy of this expression is assessed for a wide range of materials including metals, 2D materials and dielectrics, and it is shown how the distribution of the retrieved poles helps in characterizing the materials.

1. Introduction

The description of the permittivity of materials via analytical expressions is of fundamental interest in the field of optics and electromagnetism. Analytical models are relevant to provide simple and relevant descriptions of the interaction between materials and excitation fields.[1,2] They are also of strong interest for computational modeling and numerical methods such as time-domain numerical methods.[3,4] Besides the need of analytical description of the dielectric permittivity on real frequencies, modal analysis of open systems and non-Hermitian photonics requires the description of the dielectric permittivities on the complex frequency plane.[5–9] Common tools or models rely on combinations of the Drude, Lorentz and sometimes Debye models to describe the permittivity on spectral windows extending over a few dozens of wavelengths.[10–13]

Alternatively, one can derive an expression of the permittivity (or the susceptibility) as a singularity expansion.[14,15] When real-valued fields are considered in the temporal domain, this becomes equivalent to the complex-conjugate pole-residue pairs model (ccprp),[16–19] which approximates the permittivity using a finite set of complex conjugated pairs of poles contained within or close to a spectral window of interest, with the aim of providing simple analytical expressions to numerical methods.[16,20,21]

By expressing the permittivity as the transfer function of a physical system, we generalize these approaches and show that the singularity expansion method (SEM)[22,23] is the natural way to obtain an exact expression of the permittivity. The SEM can be recast into a form including the Drude, Lorentz, and Debye models which we refer to as the generalized Drude–Lorentz model (GDL). We discuss in particular what the additional terms appearing in the generalized Lorentz model translates into when we revert back to the temporal domain. We propose an approach to retrieve the parameters of the GDL model. It is an optimization method relying on the auto-differentiation tools from current machine-learning libraries, and more specifically PyTorch.[24] We test this approach and show its accuracy with experimental data corresponding to the dielectric permittivity of nine materials including metals, dielectrics and 2D materials. Finally, we show how the distribution of the poles associated with Debye, Drude, or Lorentz terms can characterize the behavior of the material at different frequencies. While we focus on non-magnetic, isotropic media for simplicity but also and mainly because these account for most of the regularly encountered media, the study presented in this work can also be applied to non-isotropic media with tensors for both the permittivity and the permeability.

2. Singularity Expansion of the Permittivity

2.1. Drude–Lorentz Model

The dielectric permittivity is often expressed as a combination of the Lorentz, Debye, and Drude models. The Debye model

I. Ben Soltane, F. Dierick, B. Stout, N. Bonod
Aix Marseille Univ
CNRS
Centrale Marseille, Institut Fresnel
Marseille 13013, France
E-mail: isam.ben-soltane@fresnel.fr; nicolas.bonod@fresnel.fr

The ORCID identification number(s) for the author(s) of this article can be found under https://doi.org/10.1002/adom.202400093

DOI: 10.1002/adom.202400093

Figure 1. The linear dielectric permittivity of a material is defined in the constitutive relations by a transfer function linking the output displacement field $\vec{D}$ to the input electric field $\vec{E}$. It shares the properties of a linear transfer and can be analytically expressed using the singularity expansion method.

being a special case of the Drude model, we will focus on Drude and Lorentz models. The Lorentz model is often used to model the behavior of the electric charges of a medium excited by an electromagnetic-field. It leads to an expression of the permittivity as a sum of N_e Lorentz functions, each associated with a group of electric charges possessing a different behavior. The Drude model describes free charges in a metal or a gas of charged particles. By simply putting them together, we obtain the classical Drude–Lorentz (DL) model

$$\mathcal{E}(\omega) = \varepsilon_0\left(\mathcal{E}_\infty - \frac{\omega_b^2}{\omega^2 + \mathrm{i}\omega\gamma} - \sum_{m=1}^{N_e}\frac{\omega_{\mathrm{p},m}^2}{(\omega^2 - \omega_{0,m}^2) + \mathrm{i}\omega\Gamma_m}f_m\right) \tag{1}$$

The Drude term is characterized by its plasma frequency ω_b and γ which corresponds to a friction-like term acting on the free charged particles within the medium. The N_e Lorentz terms have a similar expression, but are associated with forces acting upon bound charged particles. They mainly differ by the presence of the frequency $\omega_{0,m}$ which is associated with a spring-like force restoring the particles to their equilibrium position. N_e usually ranging from 1 and 5, with the usual convention that $\sum_{m=1}^{N_e} f_m = 1$, which corresponds to N_e groups of charged particles with different behaviors[25]

2.2. The Dielectric Permittivity as a Transfer Function

The permittivity $\mathcal{E}(\omega)$ is defined by the constitutive equation linking the electric field $\vec{E}$ to the displacement field $\vec{D}$. It has the form of a tensor and can be reduced to a scalar in isotropic media. The elements of this tensor link components of the exciting electric field to the components of the displacement field. Each component of the dielectric tensor behaves as a transfer function of a physical system. Transfer functions of linear and time invariant systems permit to retrieve the output field, here the displacement field $\vec{D}$, when the physical material is excited by an incoming field, here the electric field $\vec{E}$ (see **Figure 1**). In this study, we will consider isotropic, non-magnetic, linear and time invariant optical materials for which the dielectric permittivity reduces to a scalar that is obtained by taking the square of the refractive index $n(\omega)$.

The singularity expansion method has been developed to expand the transfer functions in terms of their complex singularities.[14,22,23,26–28] Under the assumptions described in Equations (S3)– (S7), Supporting Information, it yields

$$\mathcal{E}(\omega) \approx \mathcal{E}_{\mathrm{NR}} + \sum_{\ell=1}^{M}\frac{r_{\mathrm{I}}^{(\ell)}}{\omega - \omega_{\mathrm{I}}^{(\ell)}} + \sum_{\ell=1}^{N}\left[\frac{r_{\mathrm{p}}^{(\ell)}}{\omega - \omega_{\mathrm{p}}^{(\ell)}} - \frac{\overline{r}_{\mathrm{p}}^{(\ell)}}{\omega + \overline{\omega}_{\mathrm{p}}^{(\ell)}}\right] \tag{2}$$

where $r_{\mathrm{p}}^{(\ell)}$ (resp. $r_{\mathrm{I}}^{(\ell)}$) is the residue of $\mathcal{E}$ at the complex singularity or pole $\omega_{\mathrm{p}}^{(\ell)}$ (resp. imaginary pole $\omega_{\mathrm{I}}^{(\ell)}$), and $\mathcal{E}_{\mathrm{NR}}$ is the non-resonant term, a constant with a known expression depending on all the poles. Let us point out that, due to the inherent Hermitian symmetry, that is, $\overline{H(\omega)} = H(-\overline{\omega})$ of physical system resulting from the consideration of real-valued temporal signals,[29] the complex poles come in pairs $(\omega_{\mathrm{p}}^{(\ell)}, -\overline{\omega}_{\mathrm{p}}^{(\ell)})$ and so do their associated residues $(r_{\mathrm{p}}^{(\ell)}, -\overline{r}_{\mathrm{p}}^{(\ell)})$.[16,18,23]

2.3. Generalized Drude–Lorentz Expression

We now aim at demonstrating that the singularity expansion in Equation (2) can be cast into a form that encompasses the Drude–Lorentz expression in Equation (1). For that purpose, we separate three different contributions in Equation (2) regarding the position of the poles in the complex plane. In agreement with the final value theorem, we impose a pole at the origin (the detailed justification can be found in Supporting Information), and we separate the complex pairs of poles from the poles on the imaginary axis, which account for the contribution of (almost) free charges in the media. The purely imaginary poles, including the one at the origin, are associated with terms equivalent to the usual Drude or Debye relaxation terms as will be shown later. Let us call $\hat{\mathcal{E}}$ the expansion of $\mathcal{E}$

$$\hat{\mathcal{E}}(\omega) = \mathcal{E}_{\mathrm{NR}} + \varepsilon_0 \times\left(\frac{r_0}{\omega} + \sum_{\ell=1}^{M}\frac{r_{\mathrm{I}}^{(\ell)}}{\omega - \omega_{\mathrm{I}}^{(\ell)}} + \sum_{\ell=1}^{N}\left[\frac{r_{\mathrm{p}}^{(\ell)}}{\omega - \omega_{\mathrm{p}}^{(\ell)}} - \frac{\overline{r}_{\mathrm{p}}^{(\ell)}}{\omega + \overline{\omega}_{\mathrm{p}}^{(\ell)}}\right]\right) \tag{3}$$

where r_0 is the residue of $\mathcal{E}$ at 0. Let us stress that Equation (3) would be the exact expression of the permittivity $\mathcal{E}$ if the expansion were not truncated for numerical reasons.

The imaginary poles in the truncated singularity expansion, including 0, can be written as Drude terms. Let us consider the couple $(\omega_{\mathrm{I}}^{(\ell)}, r_{\mathrm{I}}^{(\ell)})$ of an imaginary pole and its associated imaginary residue. Setting $\gamma_l = -\mathrm{Im}(\omega_{\mathrm{I}}^{(\ell)})$ and $\omega_{b,\ell} \in \mathbb{C}$ such that $-\mathrm{i}\omega_{b,\ell}^2/\gamma_\ell = r_{\mathrm{I}}^{(\ell)}$ leads to

$$\frac{r_{\mathrm{I}}^{(\ell)}}{\omega - \omega_{\mathrm{I}}^{(\ell)}} = -\frac{\omega_{b,\ell}^2}{\mathrm{i}\gamma_\ell}\left[\frac{1}{\omega} - \frac{1}{\omega + \mathrm{i}\gamma_\ell}\right] + \frac{\omega_{b,\ell}^2}{\mathrm{i}\gamma_\ell}\frac{1}{\omega} \tag{4}$$

Finally, we give an expression of γ_0, the residue of the pole 0, taking into account r_0 and the residues of the other imaginary poles

$$\gamma_0 = r_0 - \sum_{\ell=1}^{M}\frac{\omega_{b,\ell}^2}{\mathrm{i}\gamma_\ell} \tag{5}$$

Thus, all the terms associated with the imaginary poles can be written as

$$\frac{r_0}{\omega}+\sum_{\ell=1}^{M}\frac{r_{\mathrm{I}}^{(\ell)}}{\omega-\omega_{\mathrm{I}}^{(\ell)}}=\frac{\gamma_0}{w}-\sum_{\ell=1}^{M}\frac{\omega_{b,\ell}^2}{\omega^2+\mathrm{i}\omega\gamma_\ell} \tag{6}$$

The sum over ℓ is equivalent to considering M groups of freely moving charges, each associated with different parameters γ_ℓ and $\omega_{b,\ell}$. Since $\omega_{b,\ell}^2$ can be negative, Equation (6) spans a larger set of functions than the regular Drude model written in Equation (1) and for which $\omega_{b,\ell}$ is a positive frequency.

Similarly, the terms involving the complex poles $\omega_{\mathrm{p}}^{(\ell)}$ can be written as Lorentz-like terms. For any pole $\omega_{\mathrm{p}}^{(\ell)}$, we have

$$\frac{r_{\mathrm{p}}^{(\ell)}}{\omega-\omega_{\mathrm{p}}^{(\ell)}}-\frac{\overline{r}_{\mathrm{p}}^{(\ell)}}{\omega+\overline{\omega}_{\mathrm{p}}^{(\ell)}}=2\frac{\mathrm{i}\omega\mathrm{Im}(r_{\mathrm{p}}^{(\ell)})+\mathrm{Re}(r_{\mathrm{p}}^{(\ell)}\,\overline{\omega}_{\mathrm{p}}^{(\ell)})}{\omega^2-|\omega_{\mathrm{p}}^{(\ell)}|^2-2i\omega\mathrm{Im}\,(\omega_{\mathrm{p}}^{(\ell)})} \tag{7}$$

Let us set $\omega_{0,\ell}=|\omega_{\mathrm{p}}^{(\ell)}|$ and $\Gamma_\ell=-2\mathrm{Im}(\omega_{\mathrm{p}}^{(\ell)})$, and two constants $s_{1,\ell}$ and $s_{2,\ell}$ such that $s_{1,\ell}\Gamma_l=-2\mathrm{Im}(r_{\mathrm{p}}^{(\ell)})$ and $s_{2,\ell}\omega_{0,\ell}^2=-2\mathrm{Re}(r_{\mathrm{p}}^{(\ell)}\,\overline{\omega}_{\mathrm{p}}^{(\ell)})$. The previous expression becomes

$$\frac{r_{\mathrm{p}}^{(\ell)}}{\omega-\omega_{\mathrm{p}}^{(\ell)}}-\frac{\overline{r}_{\mathrm{p}}^{(\ell)}}{\omega+\overline{\omega}_{\mathrm{p}}^{(\ell)}}=-\frac{\mathrm{i}s_{1,\ell}\omega\Gamma_\ell+s_{2,\ell}\omega_{0,\ell}^2}{(\omega^2-\omega_{0,\ell}^2)+\mathrm{i}\omega\Gamma_\ell}=\frac{P_{(\ell)}(\omega)}{Q_{(\ell)}(\omega)} \tag{8}$$

to provide the generalized Drude–Lorentz expression

$$\hat{\mathcal{E}}(\omega)=\mathcal{E}_{\mathrm{NR}}+\varepsilon_0\left(\frac{\gamma_0}{w}-\sum_{\ell=1}^{M}\frac{\omega_{b,\ell}^2}{\omega^2+\mathrm{i}\omega\gamma_\ell}-\sum_{\ell=1}^{N}\frac{\mathrm{i}s_{1,\ell}\omega\Gamma_\ell+s_{2,\ell}\omega_{0,\ell}^2}{(\omega^2-\omega_{0,\ell}^2)+\mathrm{i}\omega\Gamma_\ell}\right) \tag{9}$$

The N generalized Lorentz function in Equation (9) differ from the classical Lorentz functions in Equation (1) by the frequency-dependent imaginary terms $\mathrm{i}s_{1,\ell}\omega\Gamma_\ell$ in the numerator $P_{(\ell)}$ which are tantamount to non-real valued residues associated with the Lorentz poles $r_{\mathrm{p}}^{(\ell)}$. Let us look at the contribution of only one generalized Lorentz function $P_{(\ell)}/Q_{(\ell)}$ to the permittivity. The relationship between the displacement field $\vec{D}(\omega)$ and the electric field $\vec{E}(\omega)$ now reads as

$$Q_{(\ell)}(\omega)\vec{D}(\omega)=\varepsilon_0\,P_{(\ell)}(\omega)\vec{E}(\omega) \tag{10}$$

Or, by replacing $P_{(\ell)}$ and $Q_{(\ell)}$ by their expressions

$$-\left((\omega^2-\omega_{0,\ell}^2)+\mathrm{i}\omega\Gamma_\ell\right)\vec{D}(\omega)=\varepsilon_0\left(\mathrm{i}s_{1,\ell}\omega\Gamma_\ell+s_{2,\ell}\omega_{0,\ell}^2\right)\vec{E}(\omega) \tag{11}$$

It follows that the additional imaginary term $\mathrm{i}\omega\Gamma_\ell$ accounts for a new contribution of the electric field to the displacement field when we compare it to the classical Lorentz function numerator $s_{2,\ell}\omega_{0,\ell}^2$. We can perform an inverse Laplace transform of Equation (11)

$$\left((\partial_t^2+\omega_{0,\ell}^2)+\Gamma_\ell\partial_t\right)[\vec{d}](t)=\varepsilon_0\left(s_{1,\ell}\Gamma_\ell\partial_t-s_{2,\ell}\omega_{0,\ell}^2\right)[\vec{e}](t) \tag{12}$$

In the temporal domain, the imaginary term translates into a contribution of the scaled derivative of the electric field $s_{1,\ell}\Gamma_\ell\partial_t[\vec{e}](t)$ to the displacement field $\vec{d}(t)$. This new dependency can be explained via the constitutive relation linking the displacement field, the electric field, and the polarization density field $\vec{p}$: $\vec{d}=\varepsilon_0\vec{e}+\vec{p}$. The polarization density vector is connected to the electric field via the electric susceptibility. As stated in reference,[15] this is equivalent to considering two linear operators $\mathcal{L}_1$ and $\mathcal{L}_2$ such that $\mathcal{L}_1[\vec{p}](t)=\varepsilon_0\mathcal{L}_2[\vec{e}](t)$, which results in $\mathcal{L}_1[\vec{d}](t)=\varepsilon_0(\mathcal{L}_1+\mathcal{L}_2)[\vec{e}](t)$. $\mathcal{L}_1$ and $\mathcal{L}_2$ can be retrieved via identification in Equation (12)

$$\begin{aligned}\mathcal{L}_1&=\left(\partial_t^2+\omega_{0,\ell}^2\right)+\Gamma_\ell\partial_t\\(\mathcal{L}_1+\mathcal{L}_2)&=s_{1,\ell}\Gamma_\ell\partial_t-s_{2,\ell}\omega_{0,\ell}^2\end{aligned} \tag{13}$$

In the classical Lorentz approach, the last term reduces to $(\mathcal{L}_1+\mathcal{L}_2)=-s_{2,\ell}\omega_{0,\ell}^2$.

Let us combine Equations (4) and (6) to obtain the following alternative form of the truncated SEM expression

$$\hat{\mathcal{E}}(\omega)=\mathcal{E}_{\mathrm{NR}}+\varepsilon_0\left(\frac{\gamma_0}{\omega}-\sum_{\ell=1}^{M}\frac{\omega_{b,\ell}^2}{\omega^2+\mathrm{i}\omega\gamma_\ell}-\sum_{\ell=1}^{N}\frac{\mathrm{i}s_{1,\ell}\omega\Gamma_\ell+s_{2,\ell}\omega_{0,\ell}^2}{(\omega^2-\omega_{0,\ell}^2)+\mathrm{i}\omega\Gamma_\ell}\right) \tag{14}$$

Equation (14) is what we refer to as the generalized Drude–Lorentz (GDL) model as it encompasses both models (and also the Debye model) and generalizes the Lorentz terms via the additional imaginary terms. It follows that the permittivity can be equivalently approximated equivalently as a pole expansion with Equation (3), and as a GDL expression with Equation (14).

3. Retrieving the Parameters from Experimental Data

We show how to retrieve the parameters of the GDL model using experimental data at real frequencies. This approach is tested on the nine materials listed in Table S1, Supporting Information, which include oxides, metals and 2D materials.

3.1. Analytical Continuation of the Permittivity from Experimental Data

Each material is associated with a set of experimental data points $(\omega_i,\ \epsilon_i)$ with $\epsilon_i=\mathcal{E}(\omega_i)$ the permittivity measured at the real frequency ω_i. Starting from the expression of the GDL model in Equation (14), we wish to find the set of parameters $\mathcal{P}=\{\mathcal{E}_{\mathrm{NR}},\gamma_0,\omega_{b,\ell},\gamma_\ell,s_{1,\ell},\Gamma_\ell,s_{2,\ell},\omega_{0,\ell}\}$, which analytically expands the permittivity into the complex frequency plane while minimizing the distance between the experimental points ϵ_i and the estimated GDL value $\tilde{\epsilon}_{i,\mathcal{P}}=\tilde{\mathcal{E}}(\omega_i,\mathcal{P})$. The distance between the model and experimental data is defined by error or loss function L

$$\mathcal{P}^*=\arg\min_{\mathcal{P}}L(\epsilon_i,\tilde{\epsilon}_{i,\mathcal{P}}) \tag{15}$$

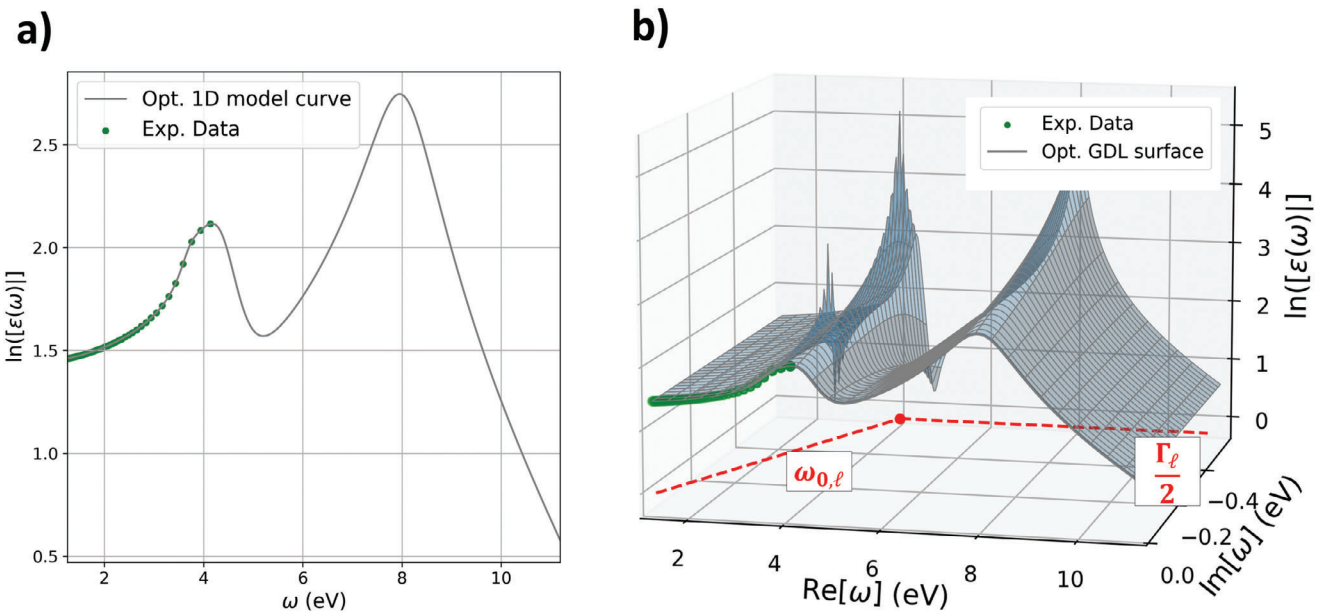

Figure 2. Optimization of a model for the dielectric permittivity of TiO_2 using experimental data. a) Classical 1D optimization by a curve that fits experimental data available at low frequencies (below 5 eV). The 1D model provides a value of the dielectric permittivity at any real frequency. b) Retrieval of the GDL parameters by auto-differentiation based on gradient-descent-like optimization. The parameters are chosen to minimize a loss function L as described in Equation (15). The process is equivalent to the optimization of a surface in the complex frequency plane by moving the poles $\omega_p^{(\ell)}$ to fit the experimental data available at real frequencies only.

The final set of parameters $\mathcal{P}^*$ is obtained with auto-differentiation, a method that has been increasingly used in optimization problems in electromagnetism thanks to the versatility and efficiency that this tool offers.[30–33] In this study, we use the open-source tools provided by the machine-learning library PyTorch. The loss function L, and the optimization process are described in Equations (S8)– (S18), Supporting Information. The analytical continuation of the permittivity using experimental data is illustrated in **Figure 2** in the case of TiO_2, where the calculated function is represented by a 1D curve at real frequencies in Figure 2a, and as a surface in the complex frequency plane in Figure 2b. Let us stress that by setting the coefficients $s_{1,\ell}$ to 0 in Equation (14), we end up reducing the generalized Lorentz terms to the classical Lorentz terms. To justify the use of the GDL model rather than the classical DL model, the two of them are compared in Figures S1 and S2, Supporting Information, where we observe that the GDL model provides more accurate expressions than the DL model when a small number of singularities are involved. This is especially true in non-metallic media. As we add more and more singularities, the models both start to account for the noise rather than the dielectric permittivity data itself, which leaves no room for comparison.

We quantify the accuracy of the approach via the calculation of the relative L_2 and L_∞ errors between the experimental data and the optimized models (see Equations (S8) and (S9), Supporting Information). The errors are summarized in **Table 1**, and show the excellent accuracy reached with the GDL model in a broad spectral range and for a large set of materials.We observe an excellent agreement of the GDL model with the experimental data for all nine materials in a large spectral window, using a very small set of poles. In addition, the GDL model outperforms the DL model due to the presence of the imaginary terms contained within the generalized Lorentz terms in Equation (8), which are required for the GDL model to comply with the SEM. Figures S1 and S2, Supporting Information support this observation by showing that the classical DL model struggles to reach the same accuracy with small sets of poles. The applicability of this expansion for a wide range of materials comes from its compliance with complex analysis required by the fact that the dielectric permittivity is a linear transfer function. We graphically highlight these results for SiO_2 and Ag in **Figure 3** where their associated GDL model are compared to the experimental data.

Table 1. Relative L_2 error ($error_2$) and L_∞ error ($error_\infty$) of the optimized GDL expressions of the permittivity for the nine materials listed in Table S1, Supporting Information. The lower the errors, the higher the accuracy. The parameters N and M represent respectively the number of generalized Lorentz terms and the number of Drude/Debye terms in Equation (14).

			Relative errors of the fitting	
Material	N	M	$Error_2$ [%]	$Error_\infty$ [%]
Au	5	1	0.272	0.247
Ag	3	2	0.854	0.964
Co	5	1	0.145	0.070
Cr	3	1	0.542	0.834
HfO_2	2	0	0.074	0.276
SiO_2	2	0	0.287	1.192
TiO_2	3	0	0.237	0.763
Ta_2O_5	6	0	0.515	1.180
Graphene	5	1	0.331	0.843

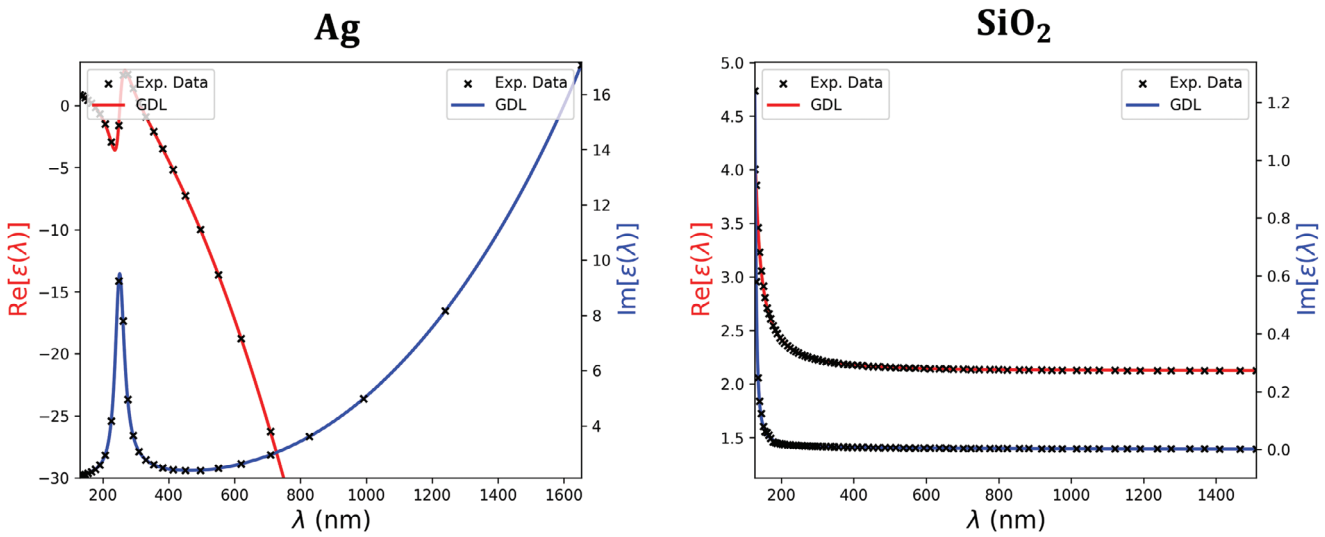

Figure 3. Real (red line, left axis) and imaginary (blue line, right axis) parts of the permittivity functions of Ag and SiO_2 calculated with the optimized GDL model (full line) and compared to the experimental data (dotted line). The permittivity functions are expressed as functions of the wavelength instead of the frequency, to better highlight the spectral windows of the experimental data ranging from the UV to the NIR. The amplitude of the permittivity of Ag quickly increases for wavelength above 380 nm, in agreement with its metallic behavior. In the case of SiO_2, the permittivity is quasi-constant in the whole spectral window, with an imaginary part close to 0 as one would expect in an absorption-free dielectric material.

3.2. Characterization of the Materials with the Distribution of the Poles

By inverting the relations introduced in Equations (6) and (4), we convert the Debye, Drude, and generalized Lorentz terms back into complex poles and residues which are then highlighted in the complex frequency plane. The poles and residues which do not contribute to significantly improving the matching between the model and the experimental data mostly help in fitting experimental or numerical noise and are therefore removed. The numbers of imaginary poles M and pairs of poles N are given in Table 1. We plot in **Figure 4** the log-amplitude of the permittivity of Au and TiO_2 in the complex frequency-plane and show qualitatively the correlation between the distribution of the poles and the amplitude of the permittivity at real frequencies.

At first glance, the real part of the poles is a good indicator of resonances and anti-resonances phenomena at real-frequencies. The distribution of the poles can be used to directly assess the behavior of the material, that is, dielectric or metal, as one would expect. Let us first consider the case of gold (Au). At low frequencies, the free electrons of the metal allow for a great reflectivity, and thus a high amplitude of the permittivity, and in particular a real part far below −1. This observation is associated with the presence of Drude poles on the imaginary axis along with a singularity at the origin. After 2.7 eV, which corresponds to approximately 430 nm, the material starts behaving like a dielectric with a rapidly varying and sign-changing real part. This phenomenon occurs at the real frequency of the first Lorentz pole. In low-absorption dielectrics such as TiO_2, the imaginary part of the permittivity is close to 0, and the permittivity is quasi-constant on a wide spectral window. In this case, the Lorentz poles are located far from that window, and thus weakly affect them. Overall, the Lorentz poles mostly mark the transitions between the different regimes, that is, the metallic regime, the dispersive dielectric regime, and the near-constant regime, while the Drude poles are associated with extremely high values of the permittivity due to the free charged particles within a metal. Therefore, it is possible to characterize the nature of the materials based on the position the poles.

Table 2. Parameters of the optimized GDL expression from Equation (14) obtained via auto-differentiation for the permittivity of Au. The frequencies $\omega_{0,\ell}$ are the moduli of the Lorentz poles, and are thus systematically larger than the imaginary parts Γ_ℓ of the poles. Since Au is a metal, the coefficient γ_0 is null, and only the Drude terms remain instead of the Drude/Debye terms. $-i\gamma_\ell$ are purely imaginary Drude poles, while the frequencies $\omega_{b,\ell}$ appear in the residues associated with the poles and are related to the frequency range within which the material still behaves as a metal.

Au				
Drude/Debye terms				
M	$\omega_{b,\ell}$ [eV]			γ_ℓ [eV]
1	6.0e+00+0.0e+00j			1.8e−02
Lorentz terms				
N	$s_{1,\ell}$	Γ_ℓ [eV]	$\omega_{0,\ell}$ [eV]	$s_{2,\ell}$
1	−9.0e−01	3.0e-01	2.7e+00	1.4e−01
2	−2.1e+00	1.4e+00	3.0e+00	2.7e+00
3	−3.6e+00	1.3e+00	3.7e+00	6.9e−01
4	−7.9e−01	5.4e+00	5.4e+00	9.5e−02
5	2.3e+00	1.9e+00	1.3e+01	5.3e−01
Non-resonant term				
ε_{NR}				4.7e−01

The values of the poles put forth in Figure 4 for Au and their associated residues are presented in **Table 2**. The moduli of the

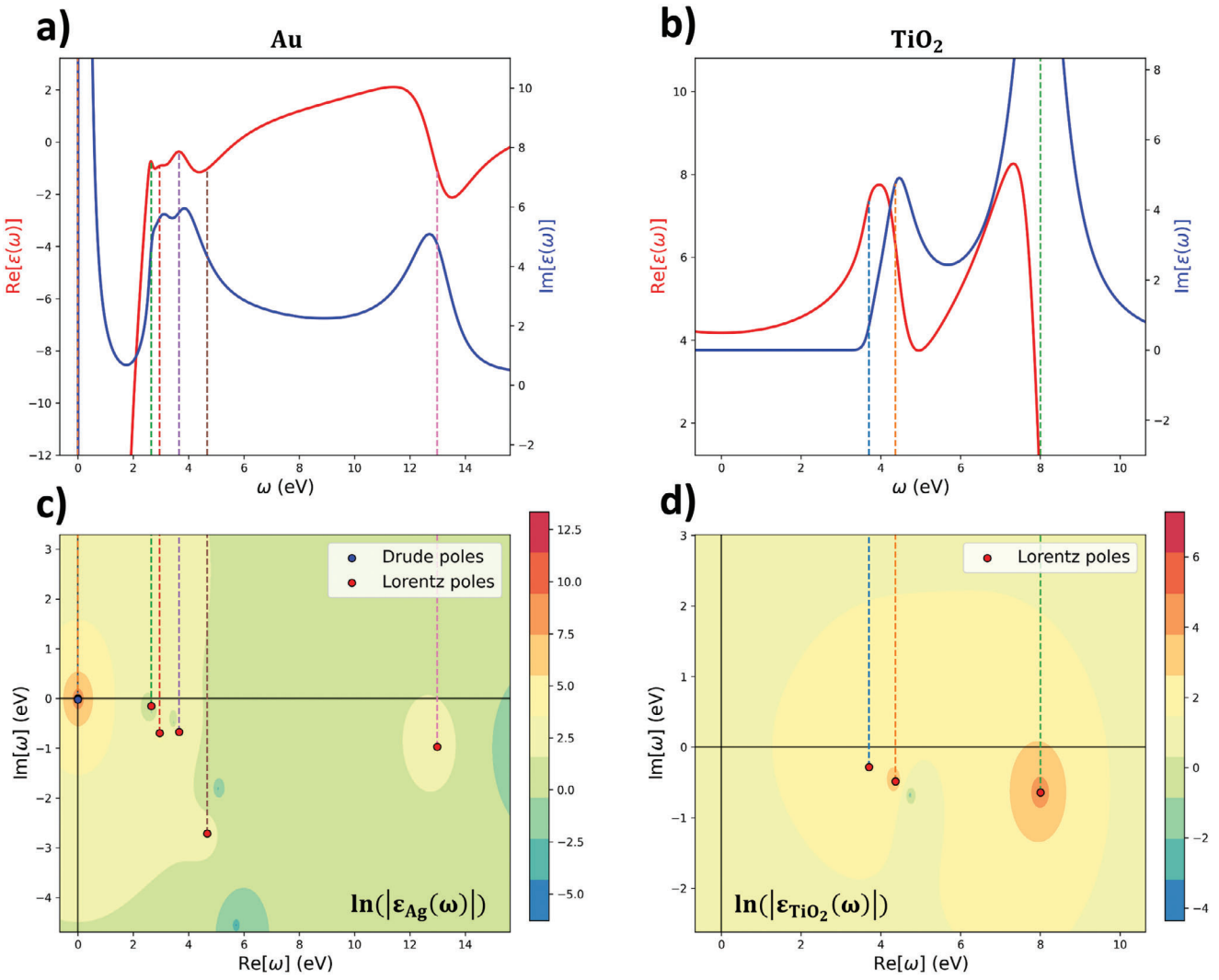

Figure 4. a,b) Real and imaginary parts of the permittivity of Au (a) and TiO_2 (b) at real frequencies, calculated using the optimized GDL. c,d) Log-amplitudes of the dielectric permittivity function in the complex frequency plane obtained with the GDL model. The poles associated with Lorentz or Drude terms are indicated by red dots in the complex ω-plane. Vertical dashed lines highlight the link between the real parts of the poles and the spectral features of the real and imaginary parts of the dielectric permittivity at real frequencies.

Lorentz poles $\omega_{0,\ell}$ located in the studied frequency window (≈1–10 eV) are in concordance with the tabulated band gaps found in the literature,[34] which goes to show that the retrieved poles hold information regarding the behavior of the materials at the microscopic scale and below.

4. Conclusion

To conclude, the dielectric permittivity is a transfer function that is naturally described by its singularity expansion in the harmonic domain, which encompasses the ccprp method. We have shown that this expansion can be recast into a generalized Drude–Lorentz model, which fully complies with the requirements and constraints of physical systems. The generalized Lorentz model, in particular, contains an additional frequency-dependent imaginary term which corresponds to a contribution of the first derivative of the electric field to the displacement field in the temporal domain. This additional imaginary term is associated with a complex residue if the harmonic domain, which sets the generalized Lorentz terms apart from the classical Lorentz terms. We have proposed a method relying on auto-differentiation to retrieve the parameters of the generalized Drude–Lorentz model and have applied it to the retrieval of the permittivity of nine different materials including oxides, metals and 2D materials. We systematically obtained very low errors using a small set of Drude and generalized Lorentz terms in a wide spectral window extending from the UV to the NIR, showcasing not only the efficiency of the method, but also the high-accuracy of the generalized model. Finally, we have shown that, by converting back the parameters of the generalized Drude–Lorentz model into poles and residues, it is possible to characterize a medium via the distribution of singularities of the permittivity. Drude singularities are associated with a singularity at the origin and purely imaginary poles and residues very close

to the origin. In transparent medium, a near-constant permittivity over a frequency range translates into a lack of singularities into and close to the associated complex frequency window. The transition from one regime to another (for instance metallic to dielectric behavior) comes along with a Lorentz pole with a relatively small imaginary part corresponding to a resonance phenomenon, hence a rapidly varying permittivity. Far from only adding degrees of freedom in the generalized Drude–Lorentz model, the imaginary parts of the residues associated with Lorentz poles are what allows the expression of the permittivity to be so accurate with so few of singularities.

Supporting Information

Supporting Information is available from the Wiley Online Library or from the author.

Acknowledgements

This work was funded by the French National Research Agency ANR Project DILEMMA (ANR-20-CE09-0027). The authors thank Guillaume Demesy for the fruitful discussions and remarks.

Conflict of Interest

The authors declare no conflict of interest.

Data Availability Statement

The data that support the findings of this study are openly available in Zenodo at https://doi.org/10.5281/zenodo.8215301, reference number 8215301.

Keywords

complex analysis, dielectric permittivity, optical materials, singularity expansion method

Received: January 10, 2024
Published online: February 24, 2024

[1] F. Andreoli, M. J. Gullans, A. A. High, A. Browaeys, D. E. Chang, *Phys. Rev. X* **2021**, *11*, 011026.
[2] H. Shim, F. Monticone, O. D. Miller, *Adv. Mater.* **2021**, *33*, 2103946.
[3] K. S. Kunz, R. J. Luebbers, *The Finite Difference Time Domain Method for Electromagnetics*, CRC Press, Boca Raton, FL **1993**.
[4] A. Taflove, *Computational Electromagnetics*, Springer, Berlin, Heidelberg **1995**.
[5] J.-H. Park, A. Ndao, W. Cai, L. Hsu, A. Kodigala, T. Lepetit, Y.-H. Lo, B. Kanté, *Nat. Phys.* **2020**, *16*, 462.
[6] Q. Song, M. Odeh, J. Zúñiga-Pérez, B. Kanté, P. Genevet, *Science* **2021**, *373*, 1133.
[7] R. Colom, E. Mikheeva, K. Achouri, J. Zuniga-Perez, N. Bonod, O. J. Martin, S. Burger, P. Genevet, *Laser Photonics Rev.* **2023**, *17*, 2200976.
[8] C. Wang, Z. Fu, W. Mao, J. Qie, A. D. Stone, L. Yang, *Adv. Opt. Photonics* **2023**, *15*, 442.
[9] C. Ferise, P. del Hougne, S. Félix, V. Pagneux, M. Davy, *Phys. Rev. Lett.* **2022**, *128*, 203904.
[10] K. E. Oughstun, N. A. Cartwright, *Opt. Express* **2003**, *11*, 1541.
[11] A. Vial, A.-S. Grimault, D. Macías, D. Barchiesi, M. L. de la Chapelle, *Phys. Rev. B* **2005**, *71*, 085416.
[12] A. Vial, T. Laroche, *Appl. Phys. B* **2008**, *93*, 139.
[13] T. Gharbi, D. Barchiesi, S. Kessentini, R. Maalej, *Opt. Mater. Express* **2020**, *10*, 1129.
[14] V. Grigoriev, G. Demésy, J. Wenger, N. Bonod, *Phys. Rev. B* **2014**, *89*, 245102.
[15] M. Garcia-Vergara, G. Demésy, F. Zolla, *Opt. Lett.* **2017**, *42*, 1145.
[16] M. Han, R. Dutton, S. Fan, *IEEE Microwave Wireless Compon. Lett.* **2006**, *16*, 119.
[17] M. Han, Z. Yu, S. Fan, in *Numerical Simulation of Optoelectronic Devices*, IEEE, Piscataway, NJ **2010**, pp. 113–114.
[18] H. S. Sehmi, W. Langbein, E. A. Muljarov, *Phys. Rev. B* **2017**, *95*, 115444.
[19] C. Warner, L. Markley, K. J. Chau, *arXiv:2209.15603* **2022**.
[20] H. Lin, M. F. Pantoja, L. D. Angulo, J. Alvarez, R. G. Martin, S. G. Garcia, *IEEE Microwave Wireless Compon. Lett.* **2012**, *22*, 612.
[21] K. P. Prokopidis, D. C. Zografopoulos, *IEEE Microwave Wireless Compon. Lett.* **2018**, *28*, 1068.
[22] C. E. Baum, *Interact. Note* **1971**, *88*, 11.
[23] I. B. Soltane, R. Colom, F. Dierick, B. Stout, N. Bonod, *New J. Phys.* **2023**, *25*, 103022.
[24] A. Paszke, S. Gross, S. Chintala, G. Chanan, E. Yang, Z. DeVito, Z. Lin, A. Desmaison, L. Antiga, A. Lerer, in Proceedings of the 31st Conference on Neural Information Processing Systems, ACM, New York **2017**, pp. 1–4.
[25] J. D. Jackson, in *Classical Electrodynamics*, 3rd edition, Wiley, New York **1999**, pp. 309–314.
[26] V. Grigoriev, A. Tahri, S. Varault, B. Rolly, B. Stout, J. Wenger, N. Bonod, *Phys. Rev. A* **2013**, *88*, 011803.
[27] R. Colom, R. McPhedran, B. Stout, N. Bonod, *Phys. Rev. B* **2018**, *98*, 085418.
[28] I. Ben Soltane, R. Colom, B. Stout, N. Bonod, *Laser Photonics Rev.* **2023**, *17*, 2200141.
[29] H. M. Nussenzveig, in *Causality and Dispersion Relations*, Mathematics in Science and Engineering, (Ed.: H. Nussenzveig), Vol. *95*, Elsevier, New York **1972**, pp. 3–53.
[30] M. Minkov, I. A. D. Williamson, L. C. Andreani, D. Gerace, B. Lou, A. Y. Song, T. W. Hughes, S. Fan, *ACS Photonics* **2020**, *7*, 1729.
[31] G. Alagappan, C. Png, *Sci. Rep.* **2023**, *13*, 4450.
[32] S. So, J. Mun, J. Park, J. Rho, *Adv. Mater.* **2022**, *35*, 2206399.
[33] S. So, J. Kim, T. Badloe, C. Lee, Y. Yang, H. Kang, J. Rho, *Adv. Mater.* **2023**, *35*, 2208520.
[34] T. Rangel, D. Kecik, P. E. Trevisanutto, G.-M. Rignanese, H. Van Swygenhoven, V. Olevano, *Phys. Rev. B* **2012**, *86*, 125125.